ISSN 1330-3651
UDC/UDK 624.137.5:519.863

# GLOBAL OPTIMIZATION OF FREEFORM SUPPORT STRUCTURES

*Simon Kulovec, Leon Kos, Jože Duhovnik*

Original scientific paper

The trends in current architectural design are leading towards structures with free and irregular forms. The connection between the design intent and the fabrication presents a challenge when creating a support structure that is geometrically viable and should possess certain aesthetics, fabricational, thermal and strength requirements. To ensure the contact of edges of neighborhood insulation panels along their thickness, their edges must be cut under different angles which cause the differences in vertex heights and further the differences of the positions of the inner metal sheets of the insulation panels. The main goal of the presented research is the development of the optimization procedure by which the minimal joint height differences will be achieved in all the joints, taking into account all free form surfaces of the individual architectural design. To compensate for the residual joint height differences the usage of spacers of different thicknesses is proposed. Quad-dominant meshes with conical properties require optimization of the vertex heights to align all beams at approximately minimal joint height differences. The paper considers global minimization of joint height differences for a sample of free form architectural design, meshed with quad-dominant mesh with conical properties. The comparison of the joint height differences before and after the optimization shows the substantial improvement.

***Keywords:*** *conical mesh, height differences minimization, offset mesh, structural optimization, support structure*

## Globalna optimizacija potpornih konstrukcija slobodnih oblika

Izvorni znanstveni članak

Postojeći su arhitektonski projekti usmjereni konstrukcijama slobodnih i neodređenih oblika. Veza između onoga što se želi postići projektom i izrade predstavlja izazov kod izvedbe potporne konstrukcije koja je geometrijski održiva, a trebala bi zadovoljiti određene estetske, izvedbene, toplinske zahtjeve i one koji se odnose na čvrstoću. Kako bi se osigurao kontakt rubova dodirnih izolacijskih panela cijelom njihovom debljinom, rubovi moraju biti odrezani pod različitim kutovima što dovodi do razlika u visini vrhova kuta te razlika u položaju unutarnjih metalnih ploča izolacijskih panela. Osnovni cilj predstavljenog istraživanja je razvoj postupka optimizacije pomoću kojega će se postići minimalna razlika u visini spoja kod svih spojišta, uzimajući u obzir sve površine slobodnog oblika pojedinog arhitektonskog projekta. Da bi se nadoknadile zaostale razlike u visini spojeva predlaže se korištenje držača razmaka različitih debljina. Mreže uglavnom četverokutne strukture konusnih svojstava zahtijevaju optimizaciju visine vrhova kutova kako bi se kod svih greda postigle približno minimalne razlike u visini spojeva. U članku se razmatra globalna minimizacija razlika u visini spojeva na uzorku arhitektonskog projekta slobodnog oblika, s mrežom uglavnom četverokutne strukture s konusnim svojstvima. Usporedba razlika u visini spojeva prije i poslije optimizacije pokazuje znatno poboljšanje.

***Ključne riječi:*** *konstrukcijska optimizacija, konusna mreža, minimizacija razlika visine, offset mreže, potporna konstrukcija*

## 1 Introduction

In architectural design, freeform structures by definition represent an area of full creativity that does not limit the architect to the use of regular shapes. In a physical realization of the project, arbitrary shapes designed by the architect must satisfy a number of requirements that limit possible realizable solutions to the final "free forms". Those are greatly used in "sculptural" designs like museums and towers that propose to be city landmarks. However, there is also large commercial interest for freeform buildings with tight budgets. Such designs seek their representation through shape, while applying cost effective materials and making use of the whole available area.

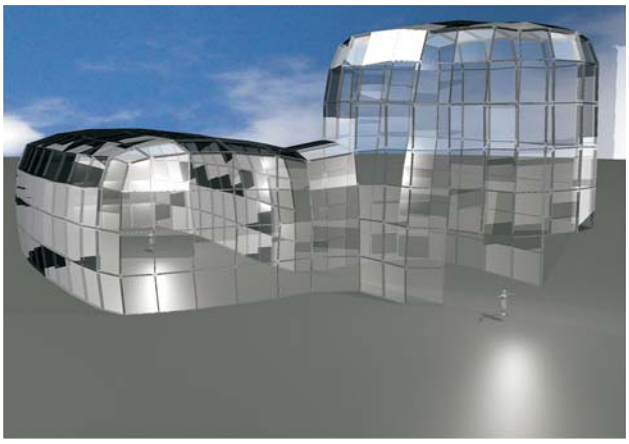

**Figure 1** Freeform surface with planar quad-dominant mesh

Freeform surfaces of the structures can be described by different types of meshes providing the planarity of each of the mesh surface elements – faces. The existing freeform structures mainly consist of triangular meshes, where the condition of planarity is satisfied automatically. We chose a quadrilateral meshes [1] because they are cost effective and simpler to construct but are geometrically complex. The condition of planarity is satisfied by optimization algorithm based on Sequential Quadratic Optimization [6].

The main mesh elements are described as the vertices, the edges and the faces (Fig. 2).

Freeform façades consist of relatively thick planar panel elements and of I beams. The outer surfaces of the panel elements coincide with mesh faces. To ensure the contact of edges of neighborhood panel elements along their thickness, their edges must be cut under different angles which cause differences in edge heights and further the differences of the positions of the inner metal sheets of the insulation panels.

Where the beams have the same height the position of the beams must compensate for the above mentioned difference in positions of inner metal sheets. Because of that the relatively large joint height differences $\Delta h_{i,j}$ (Fig. 6 and Fig. 7) are necessary.

The differences in position of the I beams ensure a constant distance between the inner metal sheet and I beams of the structure producing, on the other hand the different vertex height distances $h_{i,j}$ (Fig. 6).

The aim of the research is to develop the optimization procedure by which the minimal joint height differences $\Delta h_{i,j} = h_{i,j;\mathrm{MAX}} - h_{i,j;\mathrm{MIN}}$ will be achieved for all the joint cylinders, taking into account all the faces of the considered free form architectural design. It should be pointed out that the angles $\alpha_{i,1}$ and $\alpha_{i,2}$ in all the joints are already optimal (Fig. 6 and Fig. 7) and therefore not subject to change.

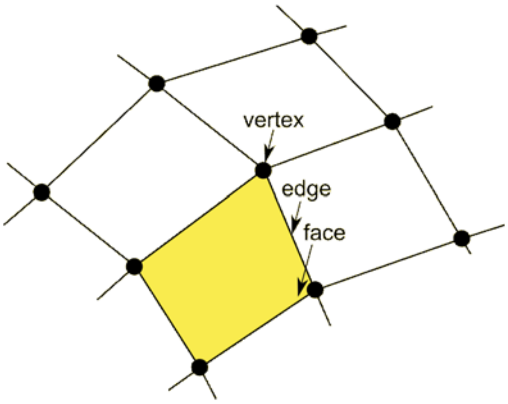


**Figure 2** Mesh elements: vertex, edge and face

To solve the optimization problem we used the *Sequential Quadratic Optimization* method [2]. Since our matrices involve many zero elements we used the *PARDISO solver* (PARallel DIrect *SOlver*) [3]. In order to speed up the optimization operation we used a parallel programming method with *OpenMP (Open Multi-Processing)* [4].

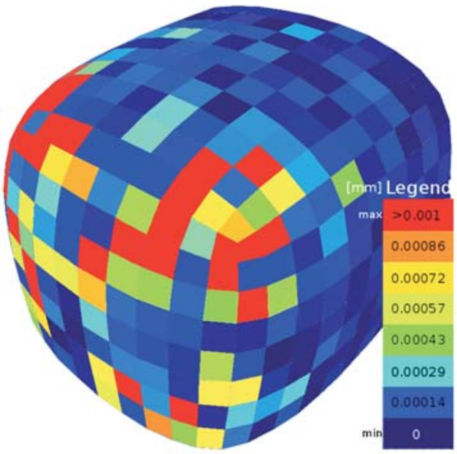


**Figure 3** (Color online) Planar pre-optimized mesh. The highest deviation of planarity is 0,16 mm. Red color presents the lowest and blue color present the highest planarity of quadrilateral mesh elements.

## 1.1 Mesh requirements

### 1.1.1 The planarity requirement

Freeform structures require planarity for each closure metal (insulation panel element) [5]. Planarity is necessary for the building of the structure, particularly in the cases when the structure is covered with non-deformable elements (e.g. glass...). We are trying to make planar elements for the selected structure while still keeping the original outside form of the structure as designed by the architect. Triangular mesh elements do not require planarization because of their geometry is always planar. Planarity of an element in a selected mesh should be executed to the level that still allows the assembly of closure elements. This primarily depends on the deformability of closure elements (Fig. 6 and Fig. 7). For a selected mesh, planarity is provided with a maximum discrepancy of 0,157 mm (Fig. 3).

### 1.1.2 The conical requirement

Advantages of conical vertices: (i) they allow offset planes of constant distance, which allows "sandwich" (composed) structures without degenerations in vertices, (ii) no geometric torsion in conical vertices, (iii) I beams have a common normal in vertices, which means no load capacity problems, (iv) a conical mesh follows the main curvatures which means that I beams' joint cylinders in vertices are mainly perpendicular to each other, and (v) Fig. 4 shows a mesh with all vertices pre-optimized to the criterion of conicality. The mesh is entirely conical when all vertices that make up the conical structure are conical.

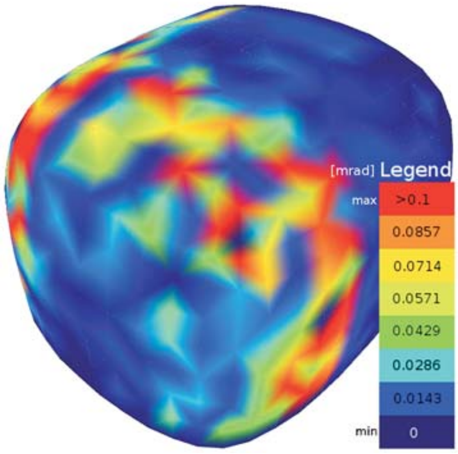


**Figure 4** (Color online) Conical pre-optimized mesh. Red color presents the lowest and blue color present the highest conicality of quadrilateral mesh elements.

## 1.2 Problem formulation

Fig. 5 shows a CAD model, designed according to planar and conical pre-optimized mesh. Fig. 5 shows the support structure only; composed of joint cylinders and I beams.

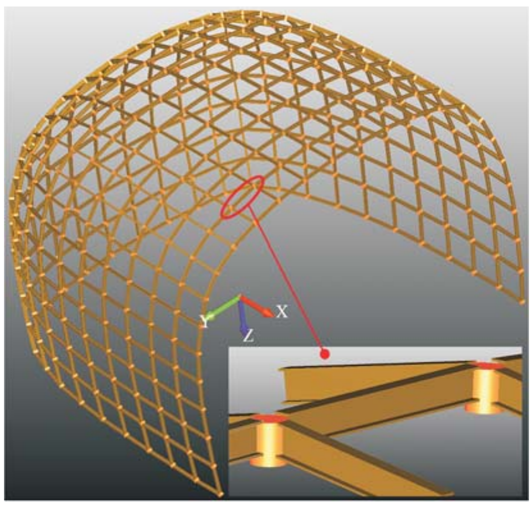


**Figure 5** CAD model of a support structure for a conical and planar mesh structure.

In every single joint cylinder is positioned according to a maximum vertex height distance ($h_{i,j;\mathrm{MAX}}$).

Therefore the top flange of the corresponding beam is leveled with the top edge of the joint cylinder. All the other I beams, having smaller vertex height distances, must be positioned higher, producing additional internal loading in the joint cylinder and joint cylinder-beam connection problems.

The idea is to provide minimal possible joint height differences ($\Delta h_{i,j}$), between top flange of the I beams in every single joint cylinder, which significantly reduces additional forces and moments in a joint cylinder (Fig. 6).

An optimization algorithm was created to do the task for all the joints in the structure.

In Section 3, a graphical analysis of joint height differences is made for the entire mesh of the sample free form structure. Minimization of these differences in particular joint significantly reduces additional forces and moments in a joint cylinders.

### 1.3. Related work

Multi-layer architecture, including conical meshes was discussed by Pottmann [7, 8] where also planar hex meshes (P-hex) were introduced. Although visually appealing, P-hex meshes were also extended to meshes with parallel edges. P-hex geometry inherits similar problems with a physical realization of vertex. The minimization of height differences can be achieved with Koebe polyhedra [9], however, this brings very restrictive geometry, which cannot approximate arbitrary shapes. Pottmann also suggests approximating beam distances with fairness functional during vertex perturbation [8]. So far, we are unaware of any architectural project that should use the present geometry processing ideas, as it seems that solutions need to be solved in detail in CAD before the realization is possible.

### 1.4 Contributions and overview

We propose spacers with different thicknesses that relax connectivity of the I beams in joint cylinders and connect them at minimal joint height differences $\Delta h_{i,j}$ (Fig. 6). Such an approach simplifies joint construction. Differences between I beam and insulation ($d_{i,1}$) are compensated with different spacer thicknesses (Fig. 7b). Our results show that such an approach simplifies joint cylinder construction to the level applicable for a parametric generation of the CAD models.

Sec. 2 presents the optimization procedure of minimizing joint height differences. The comparison of the joint height differences for the sample free form surface before and after optimization is shown in Sec. 3. In Sec. 4 the speed of calculation was enhanced with algorithm parallelization.

## 2 Optimization method

### 2.1 Specifying vertex element differences

In order to provide constant thickness $h_1$ (see Fig. 6) between I beam and outside closure metal, and to provide identical angles between beams relative to surface normal and vertices, beams should be placed at different heights.

In order to generate a CAD model, it is necessary to

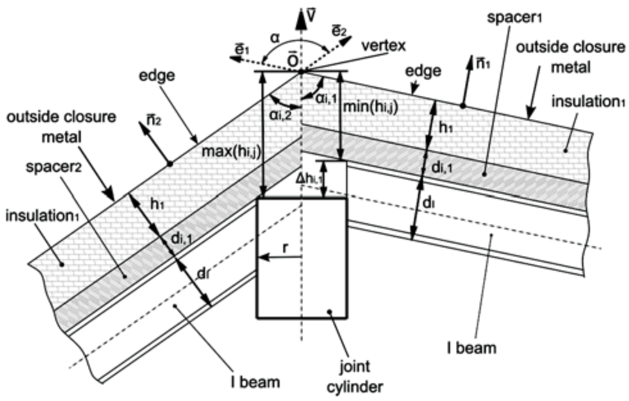


**Figure 6** Joint height differences ($\Delta h_{i,j}$) as a result of different gradients of mesh structure surfaces. $h_{i,j}$ are vertex height distance and max($h_{i,j}$) is maximal vertex height distance and min($h_{i,j}$) is minimal vertex height distance.

specify points where support structures and joint cylinders are positioned. I beams are displaced at fixing points in the joint cylinder. A box [12] or, in our case, a cylinder can be used as the joint. Calculation of I beam positions, displaced from reference points, is shown below.

Fig. 6 shows a cross-section of the cylindrical joint, beams with insulation, spacers and outside closure metal. Outside closure sheet normals $\vec{n_1}$ and $\vec{n_2}$ are joined in vertex reference point $\vec{o}$ (Fig. 6).

$$h_{i,j} = h_1 \cdot \frac{\vec{n_e} \cdot \vec{n_1}}{\| \vec{n_e} \| \cdot \| \vec{n_1} \|} + | r_e \cdot \vec{e} - \vec{r} |, \tag{1}$$

where $\vec{n_e} = \dfrac{\vec{n_1} \times \vec{n_2}}{| \vec{n_1} \cdot \vec{n_2} |}$ and $\vec{r_e} = r \cdot \dfrac{| \vec{e} | \cdot | \vec{n_e} |}{\vec{e} \times (-\vec{n_e})}$.

Vertex positioning. For each vertex $i$ of the selected mesh, vertex height distance $h_{i,j}$ (Fig. 6) is determined:

$$h_{i,j;\mathrm{MAX}} = \max(h_{1,1} + d, ..., h_{1,i} + d, ..., h_{1,n} + d), \tag{2}$$

where index $i = 1 \dots n$ represents vertices, index $j = 1 \dots m$ represents the I beams of a given mesh.

### 2.2 Determining the cost function

The cost function is created by taking into account all vertex height differences in the selected mesh.

$$F(h) = \sum_{i=1}^{n} \sum_{j=1}^{m} (| h_{i,j} - h_{i,j+1} | + | h_{i,j} - h_{i+1,j} |), \tag{3}$$

where $i = 1 \dots n$ and $j = 1 \dots m$.

Index $i$ represents the vertices, index $j$ represents I beams of a given mesh.

The first part of the cost function represents the vertex height differences ($h_{i,j}$), while the second part of the cost function represents the connection of the current vertex with the neighboring ones. Cost function compares the vertex height differences of the I beams.

## 3
## Results of global optimization

By means of global optimization we are attempting to provide minimal joint height differences while preserving the original design of the mesh. By assuring the minimal joint height difference of the I beams in the individual joint cylinder also the misalignment of the beam's axes is minimized and further the additional forces and moments originating from these misalignments are also minimized. By moving the I beams to minimal joint height distances, we avoid additional forces and momentums. The resulting shift of I beams introduces distances between the inside closure metal of the panel and the individual I beam (see $d_{i,1}$ and $d_{i,2}$ in Fig. 7b). These distances are compensated with the spacers of adapted thicknesses (Fig. 6 and Fig. 7). After optimization thickness $d_{i,1}$ is no longer a constant for all the façade but can be different for each beam, $\Delta h_{i,2} < \Delta h_{i,1} \rightarrow d_{i,2} < d_{i,1}$ (see Fig. 7b).

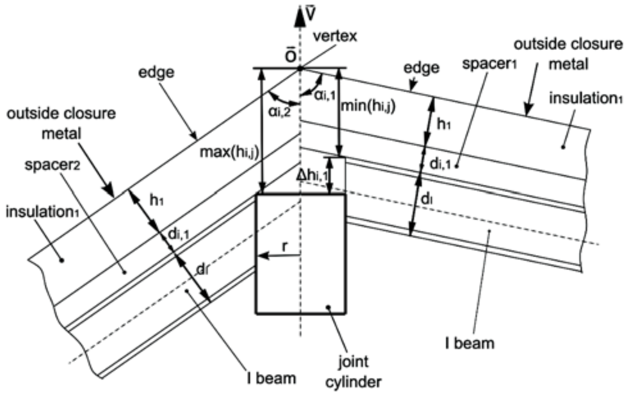


a) Initial vertex cross-section with equal spacer thickness ($h_1 + d_{i,1}$)

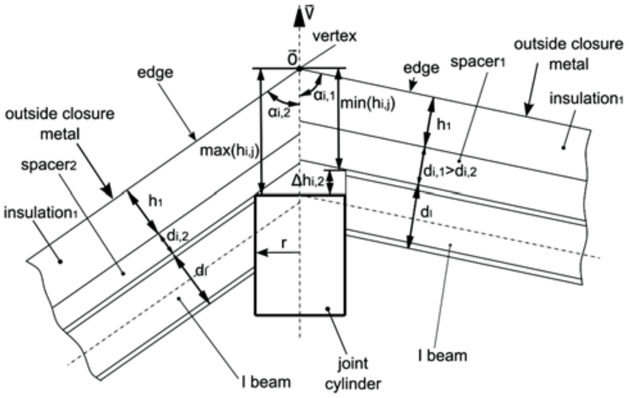


b) Post-optimized vertex cross-section with variable spacer thickness ($\Delta h_{i,2} < \Delta h_{i,1} \rightarrow d_{i,2} < d_{i,1}$)

**Figure 7** Minimized joint height differences before ($\Delta h_{i,1}$) and after ($\Delta h_{i,2}$) optimization ($\Delta h_{i,2} < \Delta h_{i,1}$)

### 3.1
### Height differences before and after optimization

We made a comparison of joint height differences before and after optimization. It can serve as a basis to characterize the optimization process.

Fig. 8 shows the convergence of the cost function (Eq. 3) that describes the problem of joint height differences $\Delta h_{i,j}$ (Fig. 6 and Fig. 7) which we would like to minimize. The cost function is composed of the sum of vertex height differences ($h_{i,j}$) for each vertex in a given mesh. A constraint, determining the interval by which each beam can move is [0,10] mm.

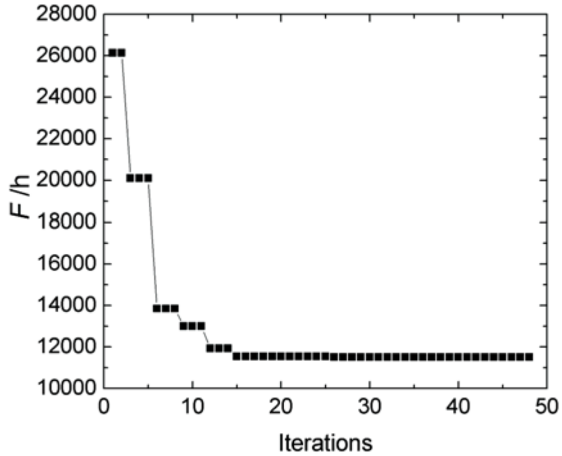


**Figure 8** Cost function (mm) convergence

In ten iterations, the cost function reaches a maximum drop, followed by reaching almost top convergence after 15 iterations and not changing significantly up to the 50$^{th}$ iteration, when it reaches the stopping criterion *epsilon* (chosen according to requirements).

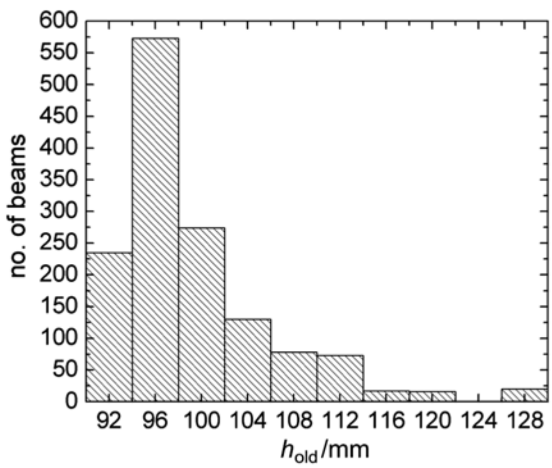


**Figure 9** Beams distance from vertices before optimization

The histogram in Fig. 9 shows the vertex height distance of a mesh before optimization. Vertex height distance is in the range [90,130] mm (Fig. 9). After optimization we have most vertex height distances in range [94,114] mm (Fig. 10).

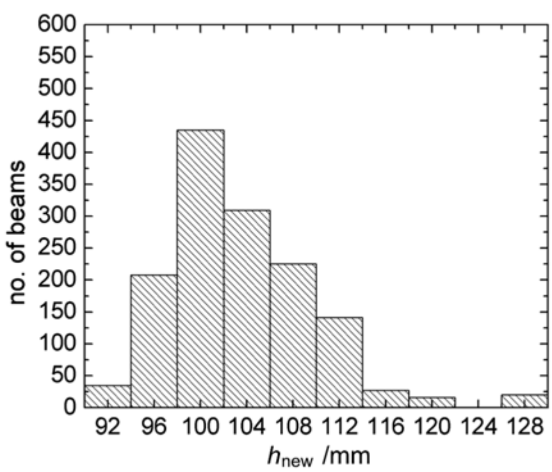


**Figure 10** Beams distance from vertices after optimization

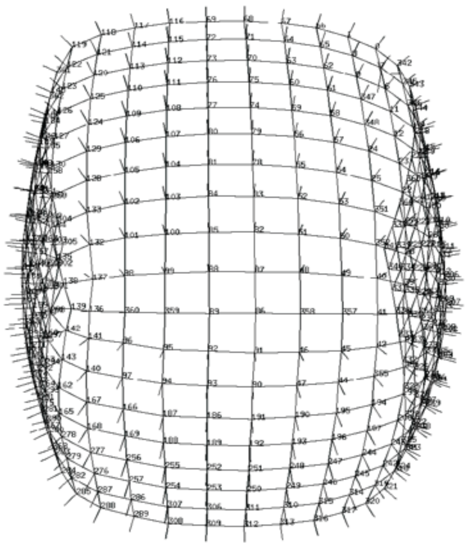

Figure 11 Upper distributions of vertices for a selected mesh

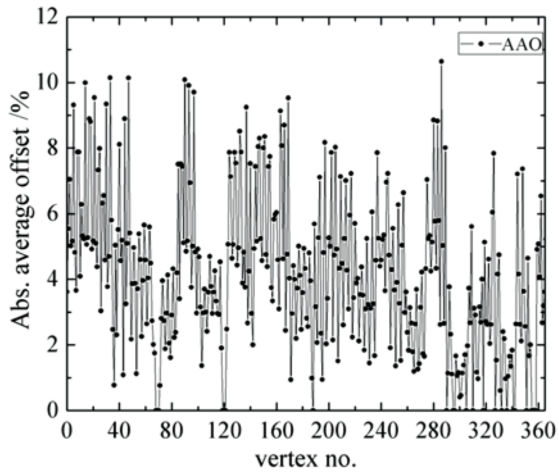


**Figure 12** Differences of average vertex height distances (*AAO*) before and after optimization,

$$AAO = \frac{h_{i,j;\text{after opt.}} - h_{i,j;\text{before opt.}}}{h_{i,j;\text{after opt.}}}$$

A more detailed distribution of all vertices is available in the *Appendix* (Fig. 18). The distribution of vertices on a mesh structure (Fig. 11) is important in order to better illustrate displacement and variations of vertex joint distances presented on the graphs.

The graph in Fig. 12 shows differences in absolute vertex height distances before and after optimization. Vertex height distances $h_{i,j}$ before and after optimization are in the range of up to a maximum of 11 %. The average of vertex height distances is 6 %. It should be pointed out that the vertices are not numbered sequentially (Figs. 11÷18). Due to large variations between vertices, this can be seen also in Fig. 12. Larger vertex height distances mainly appear on the edges of a mesh, where average distances in the range of the optimization's ceiling of 10 mm occur. Zero values on the graphs mainly represent edge vertices with only three beams.

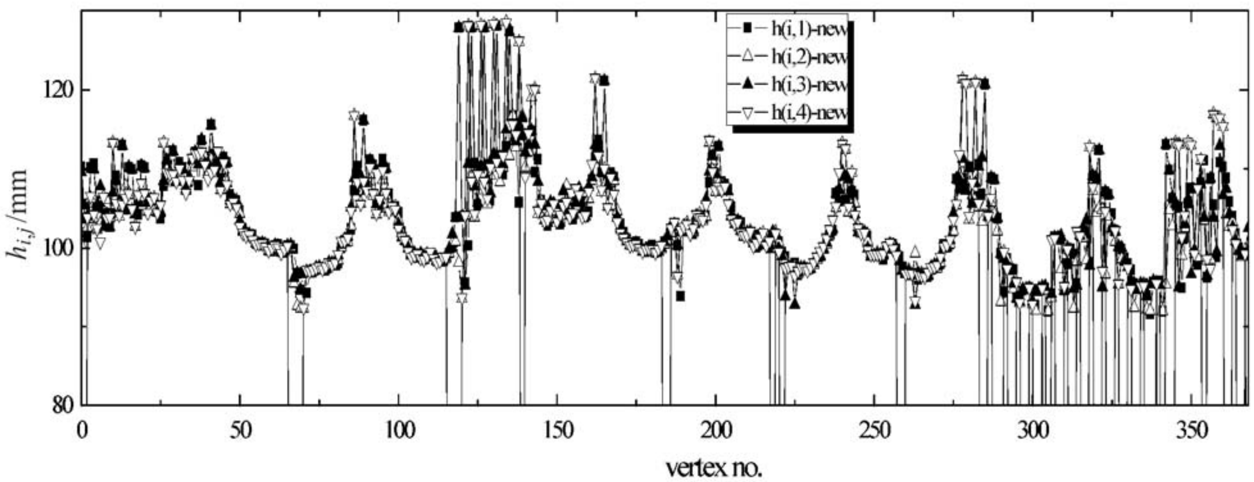


**Figure 13** Vertex height distances $h_{i,j}$ before optimization ($\sigma_{\text{before opt.}}$ = 3,06 mm)

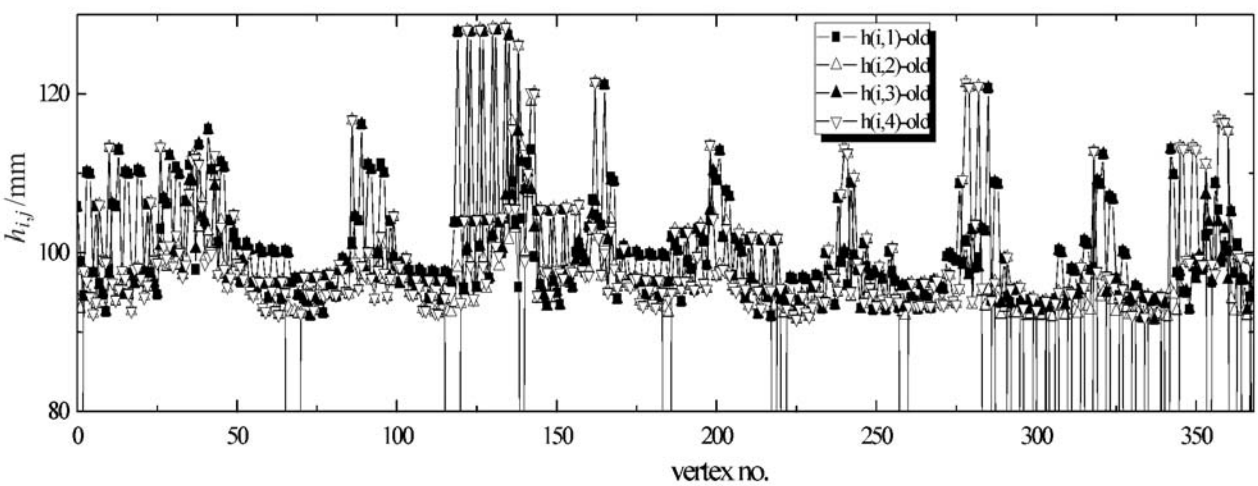


**Figure 14** Vertex height distances $h_{i,j}$ after optimization ($\sigma_{\text{after opt.}}$ = 1,29 mm)

Comparison between individual vertex height distances for every single I beam before and after optimization is shown in Figs. 13 and 14. It shows vertex height differences $h_{i,j}$ (Fig. 6) of individual beams for all the vertices of the mesh. It can be seen that the deviation of vertex height differences $h_{i,j}$ (Fig. 6 and Fig. 7) is reduced from $\sigma_{\text{before opt.}}$ = 3,06 mm before into $\sigma_{\text{after opt.}}$ = 1,29 mm after optimization. In an ideal optimization, the curves on the graph (Fig. 14) would overlap, which would mean that joint height differences $\Delta h_{i,j} = f(h_{i,j})$ of a single beam are minimal. The vertex height distances, falling under the value of 90 mm are equal to zero (boundary triangular vertices).

Fig. 14 shows that the curves of vertex height distances from the vertex improve in almost all vertices after optimization. On vertices with three I beams only; which are mostly on I beam vertices, it is not possible to achieve a quasi-ideal situation.

It can be concluded that the distribution of joint height distances ($\Delta h_{i,j}$) on the mesh is improved after optimization. Optimization brings more constant joint height distances on the mesh. We believe that is optimized mesh: (i) cost effective, and (ii) simpler to construct.

## 4 Speed up post-optimization process using *OpenMP* parallelization

Comparison of calculation speed optimization is performed on two different computers and using three different processor combinations: (i) WorkStation: *Intel© Core™2 Quad Proc. Q6600*, (ii) Prelog [Comp. Node (CPU:12)]: *Intel© Xeon© Proc. X5670*, and (iii) Prelog [Comp. − Node (CPU:24)]: *Intel© Xeon© Proc. X5670*.

We made comparisons on a *WorkStation* and on the Faculty of Mechanical Engineering's supercomputer *Prelog* (FME, UL, Slovenia). On the *Prelog* were made two comparisons with different uses of cores. *Prelog* is a supercomputer with 768 cores, 3TB of memory and 20TB of disk space. The configuration of the supercomputer's computing part consists of 64 nodes, composed of 16 frames, with each of them including 4 compute nodes in the next configuration for an individual compute node.

### Intel© Core™2 Quad Processor Q6600

Parallelization of the program source code is carried out on the work station's four processors. Processor usage in relation to speed up the optimization time is shown in Fig. 15. It can be seen that before optimization, processor usage is fewer than 10 %, which is the usage of the operating system. Once the optimization has started, processor usage on all four processors increases simultaneously, in 1 s, to around 98 %. During the speed up optimization, processor usage is in the range of 95÷100 %. Optimization of the selected mesh (Fig. 1 and 5) on high loaded processors takes 9 seconds.

### Prelog [Cumputer Node (CPU:12)]: Intel© Xeon© Processor X5670

The analysis of the 12 processors usage on one node of the *Prelog* supercomputer is shown in Figure 16. With one node containing 12 processors, full usage is expected of all of them while maintaining or reducing optimization time. From the beginning of optimization, it takes 2 s to reach full processor load. Optimization takes 5 s with the usage of processor load in range 70÷80 %.

### Prelog [Cumputer Node (CPU:24)]: Intel© Xeon© Processor X5670

At the end is shown an analysis of the usage of the 12-processor node with 12 threads on the *Prelog* supercomputer. The graph in Figure 17 shows that the usage for half of the threads exceeds 70 % while it is less than 30 % for the other half. Total utilization for all of the node's 24 threads is 50 %, which is identical to the usage of 12 cores only. Optimization takes 5 s, which is nearly 50 % faster, compared to the optimization on four cores. Judging by thread usage distribution, it can be observed that each supercomputer's node has 12 physical cores. Optimization with 24 threads makes sense in the case where the problem to be solved does not require a lot of memory. In the case of a memory-demanding problem, maximum usage of the core or threads can be in the range of 12 physical cores of the node used.

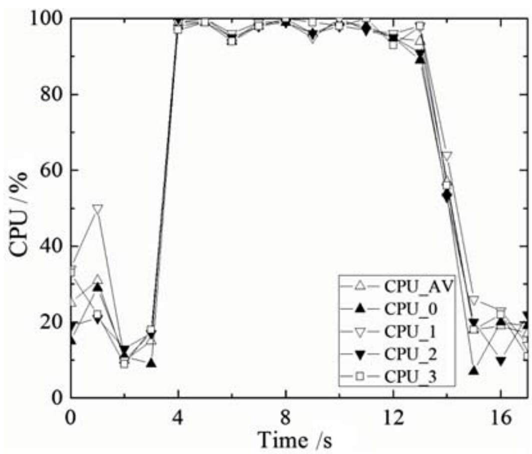


**Figure 15** Usage on 4 processors

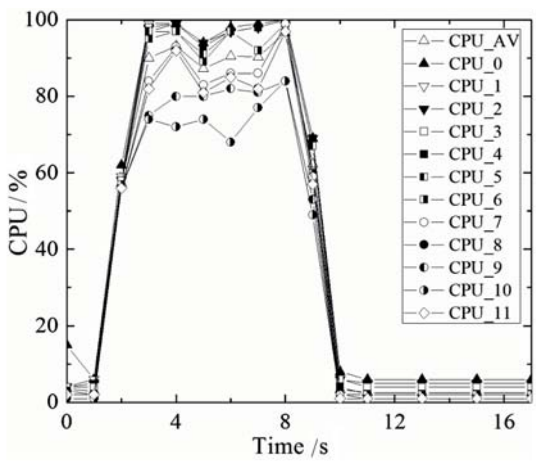


**Figure 16** Usage on 12 processors

## 5 Conclusions

We have presented the optimization of a CAD structure for any given mesh with the use of the *Intel Math Kernel* and *OpenMP*. The aim of the optimization is to provide minimal joint height differences $\Delta h_{i,2} < \Delta h_{i,1}$ (Fig. 7). The focus is on quadrilateral meshes as they are cost effective. An analysis of the initial and optimized meshes was made in order to ascertain whether the structure is improved after the optimization and whether the mesh keeps its original shape. The optimization algorithms are then speed parallelized (using *OpenMP*), and a comparison was made on the effect

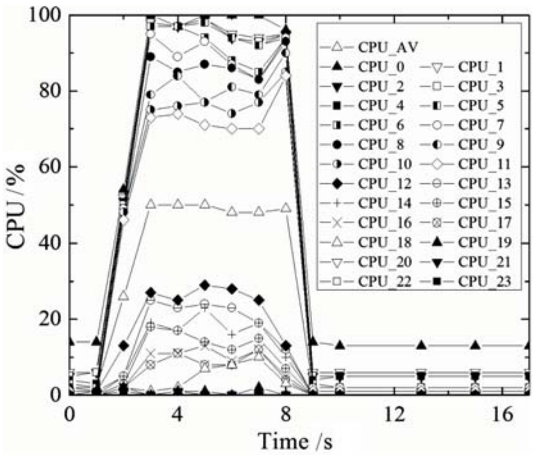


**Figure 17** Usage on 24 hyper-processors

of a larger number of processors on the speed of solving the problem of minimizing joint height differences. Computer capacities with 4, 12 processors and 24 hyper-processors were used as the benchmark (Fig. 17, 18 and 19).

The first part is represented by the optimization algorithm. It provides, globally, the minimal joint height differences for the beams in the individual vertices of a given mesh (Fig. 1). For the optimization we can rely on the *Intel Math Kernel* library, which includes tools for solving non-linear problems. The optimization tries to provide minimal joint height distances ($\Delta h_{i,j}$) which provides strength stability (additional forces and momentums in joint cylinder are minimal) of the construction. The cost function for the optimization is so structured that it keeps the original shape of any given mesh (Eq. 3).

The second part involves a mesh analysis before and after optimization. In a quasi-ideal situation the curves (Fig. 14) should overlap, which would mean that all the vertex's I beams have the minimal joint height differences. The deviation before $\sigma_{\text{before opt.}}$ = 3,06 mm and after $\sigma_{\text{after opt.}}$ = 1,29 mm optimization procedure. We believe that the optimized mesh is: (i) cost effective, and (ii) simpler to construct.

Finally, we wanted to speed up the optimization of the mesh structure. We made parallelization of the speed up optimization algorithms using *OpenMP*. For comparison, we used a *WorkStation* with four processors and a node on the *Prelog* (FME, UL, Slovenia) supercomputer with 12 processors and 24 hyper-processors. The conclusion is that the use of more processors reduces the optimization times, but not linearly (Fig. 15, 16 and 17).

## 6 References


[1] Kulovec, S.; Kos, L.; Duhovnik, J. Mesh smoothing with global optimization under constraints. // Strojniški vestnik - Journal of Mechanical Engineering, 57, 7 (2010), 555-567.

[2] Madsen, K.; Nielsen, H. B.; Tingleff, O. Optimization with constraints, 2nd edition, 2004.

[3] Schenk, O.; Gärtner, K. Solving unsymmetric sparse systems of linear equations with pardiso. // Journal of Future Generation Computer Systems, 20, 4(2004), 475-487.

[4] Chapman, B.; Jost, G.; der Pas R. V. (eds) Using, OpenMP - Portable Shared Memory Parallel Programming. The MIT Press, 2008.

[5] Wang, W.; Liu, Y.; Yan, D.; Chan, B.; Ling, R.; Sun, F. Hexagonal meshes with planar faces. Tech. Rep. TR- 2008-13, Department of Computer Science, The University of Hong Kong, 2008.

[6] Pottmann, H.; Wallner, J. The focal geometry of circular and conical meshes. // Advances in Computational Mathematics, 29, 3(2008), 249-268.

[7] Pottman, H.; Asperl, A.; Hofer, M.; Kilian, A. (eds) Architectural Geometry. Bentley institute Press, Exton, Pennsylvania USA, 2008.

[8] Pottmann, H.; Liu, Y.; Wallner, J.; Bobenko, A.; Wang, W. Geometry of multi-layer freeform structures for architecture. // ACM Trans Graphics, 26, 3(2007), 65.

[9] Bobenko, A. I.; Hoffmann, T.; Springhorn, B. A. Minimal surfaces from cycle patterns: Geometry from combinatorics. // Annals of Mathematics, 164, 1(2006), 231-264.

[10] Kos, L.; Kulovec, S.; Zaletelj, V.; Duhovnik, J. Structure generation for free-form architectural design. // Advanced engineering, 3, 2(2009), 187-194.

[11] Kos; L.; Kulovec, S.; Duhovnik, J. Support structure optimization for freeform architectural design. TMCE 2010, Delft: University of Technology, (2010), pp. 829-840.

[12] Duhovnik, J.; Kulovec, S.; Kos, L. Multiple vertex joint adapter, patent no. p201000325, 2010.



**Authors' addresses**

***Simon Kulovec***
University of Ljubljana
Faculty of Mechanical Engineering
Aškerčeva cesta 6
1000 Ljubljana, Slovenia
e-mail: simon.kulovec@lecad.uni-lj.si

***doc. dr. Leon Kos***
University of Ljubljana
Faculty of Mechanical Engineering
Aškerčeva cesta 6
1000 Ljubljana, Slovenia

***prof. dr. Jože Duhovnik***
University of Ljubljana
Faculty of Mechanical Engineering
Aškerčeva cesta 6
1000 Ljubljana, Slovenia
e-mail: joze.duhovnik@lecad.uni-lj.si

## 7 Appendix

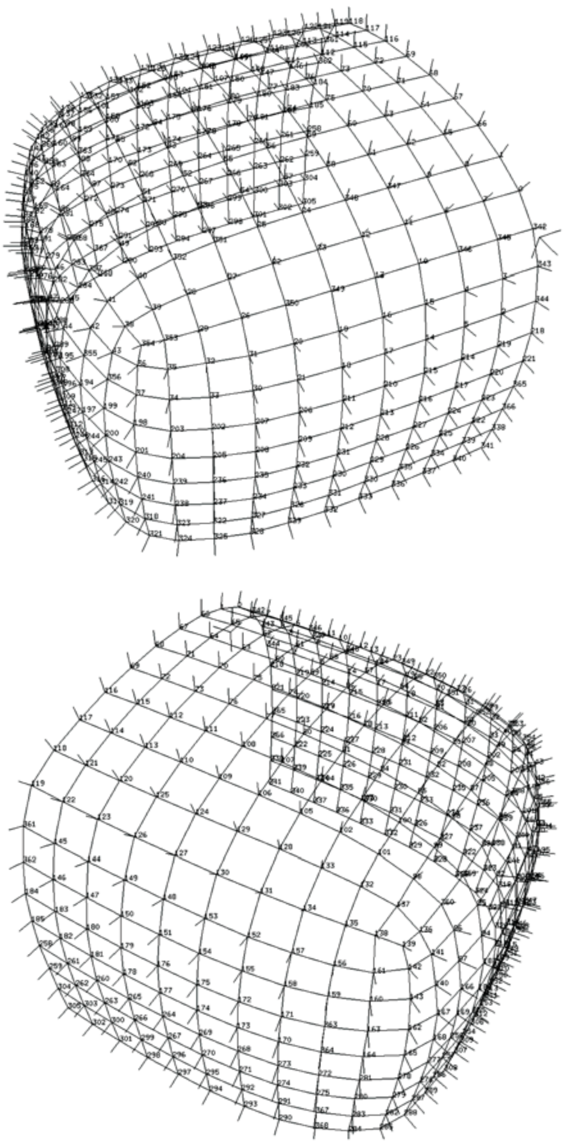

**Figure 18** Distribution of vertices for a quadrilateral mesh